

Ni nanoparticles dispersed on γ -Al₂O₃ by induced-gelation sol-gel method

M. Mónica Guraya^{#1}, Soledad Perez Catán^{*2}, Miguel D. Sánchez^{##}, and Sergio Moreno^{**}

[#] Complejo Tecnológico Pilcaniyeu, CNEA, Bustillo 9500, 8400- S.C.de Bariloche, Argentina. Universidad Tecnológica Nacional, Facultad Regional Buenos Aires-Extensión Áulica Bariloche, Argentina.

^{*} Laboratorio de Análisis por Activación Neutrónica, Centro Atómico Bariloche, CNEA, Bustillo 9500, 8400- S.C.de Bariloche, Argentina.

^{##} Departamento de Física, Universidad Nacional del Sur y Planta Piloto de Ingeniería Química (UNSCONICET), Avda Alem 1253, 8000-Bahía Blanca, Argentina.

^{**} Centro Atómico Bariloche, CONICET, Bustillo 9500, 8400- S.C.de Bariloche, Argentina.

Abstract –

A series of Ni/ γ -Al₂O₃ samples were prepared by the sol-gel method using a solution of nickel nitrate as gelation agent. The Ni content of the samples was in the range 7-39 wt%. High specific BET areas, from 150 to 200 m²/g, were determined in samples after 4 h calcination at 600 °C.

As the metal was incorporated into the alumina during formation of the porous structure, high metal-support interaction and nickel dispersion were expected. To investigate the extent of these effects, reducing treatments were carried out and monitored by Thermogravimetry (TG), Scanning Electron Microscopy (SEM), Transmission Electron Microscopy (TEM), and X-ray Diffractometry (XRD).

All XRD spectra from calcined samples showed patterns corresponding to NiO and spinel-like NiAl₂O₄ structures. Reducing treatments at 400°C were performed in a TG set up, in 10% H₂/Ar flow, until no mass change was detected. XRD spectra recorded afterwards showed Ni⁰ diffraction peaks corresponding to 20nm metal particles but also NiO and NiAl₂O₄ patterns consistent with smaller particles of 4-7 nm in size.

Subsequent treatments at 700°C also in H₂/Ar flow allowed accomplishing the metal reduction. XRD spectra indicated that reduction was complete in all samples after 30 min plateau. This time proved short enough to avoid introducing much distortion in the alumina matrix as confirmed by BET area.

All samples showed particles of 20-30 nm in size under TEM, indicating that this method allows the obtention of high dispersed Ni particles even for very high Ni contents.

Keywords: Ni/gamma-alumina, NiAl₂O₄ spinel, high dispersion Ni

I. INTRODUCTION

Ni catalysts supported on mesoporous alumina have been widely investigated for decades due to their applicability in many industrial processes

involving hydrocarbons decomposition [1]-[4]. In the last years this one and other active materials have been proposed for membranes coatings to be used in both catalytic membrane reactors and hydrogen separation [5]-[10].

Regardless the specific application involved, a general requirement of high and stable metal dispersion is demanded. This property is associated to formation of very small metal particles, which are resistant to sintering and carbon deposition in case of reforming and oxidation reactions [11]-[14]. High specific support area is also necessary when designing a catalyst or membrane coatings; for this purpose γ -Al₂O₃ is particularly suitable for moderate operation temperatures [15]-[17].

Kim et al. have studied the influence of strong metal support interaction (SMSI) [12] on the final Ni particle size, i.e. after calcination and subsequent reduction to obtain Ni⁰. Murata et al. [18] have reported that Ni/Al₂O₃ catalysts were more active and stable than the corresponding supported on Si₂O. The general agreement among authors is that nickel aluminate species produced by SMSI give nickel nanoparticles, i.e. high metal dispersion [19], [20].

Sample preparation by impregnation methods proved efficient in obtaining Ni/ γ -Al₂O₃ materials, although high metal dispersion can only be achieved with low Ni contents. Xu et al. [21] demonstrated that high metal loadings in impregnated samples led to large metal particles and, therefore, to low metal dispersion.

Sol-gel methods however, are more suitable for producing small nickel particles as many studies have established [22].

A disadvantage observed in Ni/ γ -Al₂O₃ materials, where SMSI mostly generates NiAl₂O₄ – like species, is that reduction temperature becomes high, thus resulting undesirable matrix distortion the porous alumina support, which reduces its specific area [23].

In this work we prepared a series of Ni/ γ -Al₂O₃ samples via sol-gel, where peptising was modified in order to favor the dispersion of Ni ions in

the boehmite matrix. Samples with Ni loadings in the range 9 to 39 wt% with high specific area and high nickel dispersion were obtained.

Porous structure and nickel distribution on the samples was characterised by nitrogen adsorption at liquid nitrogen temperature, Scanning Electron Microscopy (SEM), Transmission Electron Microscopy (TEM) and X-ray Diffractometry (XRD), the latter to identify nickel chemical states. Reduction process was investigated by a combination of Thermogravimetry (TG) in H₂/Ar flow, XRD, and TG- MS, with which the metal areas were determined.

II. EXPERIMENTAL

A. Sample Preparation

A boehmite colloidal suspension was prepared, following Yoldas method [24] by hydrolysis at 80°C of aluminium sec-butoxide previously prepared in our laboratory, and subsequent peptising with nitric acid, the ratio acid/boehmite being 0.07 mol/mol. Aliquots of 9.3 % solution of nickel nitrate (Fluka NiNO₃.6H₂O, 99.7 %) were incorporated to the suspension, inducing gelation in a very short time. Gels were dried at 90°C for 12 h and calcined afterwards 4h at 600°C.

Following the same procedure, a sample of γ -Al₂O₃ without Ni was prepared for comparison to support behaviour; peptising was performed by an adequate volume of HNO₃ to compensate the absence of nickel nitrate.

B. Sample Characterisation

Quantitative determinations of Al and Ni were carried out in Atomic Absorption Spectroscopy (AAS) and Scanning Electron Microscope with Energy Dispersive X-ray Analyses (SEM-EDAX).

Nitrogen adsorption-desorption isotherms at liquid nitrogen temperature were recorded in a Digisorb 2600 instrument from Micromeritics Inst. Corp.

Reducing treatments were carried out in a Netzsch STA 409 set-up in 60 cc/min H₂/Ar (1:10) flow. Powder X-ray Diffraction (XRD) measurements (15° < 2 θ < 85°) were conducted in a Philips PW1700 diffractometer with Cu α radiation and a graphite monochromator. Crystallite sizes were determined by Scherrer formula [25] from XRD data. Multi-component peaks were fitted by means of pseudo-Voigt curves to determine peak widths.

Scanning Electron Microscopy (SEM) determinations were performed in a Philips 515 scanning electron microscope with energy dispersive X-ray analyser (EDAX) Genesis 2000 whereas TEM observations were carried out in a Philips CM200UT Microscope.

III. RESULTS AND DISCUSSION

Ni content values for all samples as determined by Atomic Absorption Spectroscopy and

EDAX are presented in Table 1, where the labels assigned to samples are also indicated.

Porous structure of samples calcined at 600°C and after reducing treatments was derived from the adsorption – desorption isotherms obtained by means of nitrogen adsorption at liquid nitrogen temperature. BET surface areas for calcined and completely reduced samples are included in Table 1.

Volume pore distribution for all samples after calcination is presented in Fig. 1. The γ -Al₂O₃ support obtained in all cases, had high specific area and narrow pore distribution centered at 4nm, approximately. The centre of the pore distribution shifted towards larger diameters with Ni content, but remained below 5 nm for all samples. This suggested high porosity in the samples even for the sample with highest Ni load

Table 1 : Ni Content And Bet Areas for All Samples

Sample	AAS (wt%)	EDAX (wt%)	BET area calcined (m ² /g)	BET area reduced (m ² /g)	Metal area * (m ² /g)
γ -Al ₂ O ₃			266	229	
Ni 7	6.9	9.4	184	170	18.4
Ni 9	9.2	11.8	173	155	25.5
Ni 24	24.5	21.4	170	158	31.9
Ni 39	39.3	38.1	146	128	27.7

* indicated as m²/(g of metal)

Also regarding the porous matrix structure, results from SEM characterisation of the samples with highest Ni contents are presented in Fig. 2. Primarily, it can be seen that γ -Al₂O₃ structure is quite homogeneous, with a mean particle size of 100nm, approximately. For Ni content determination by EDAX, 200x150 μ m² was chosen as a typical analysis area; the even distribution of Ni species was tested by mapping the sample composition at many points analysing 1 μ m² regions. Ni content distribution was found homogeneous; the statistical dispersion among values determined in different regions, kept within 20% for all samples.

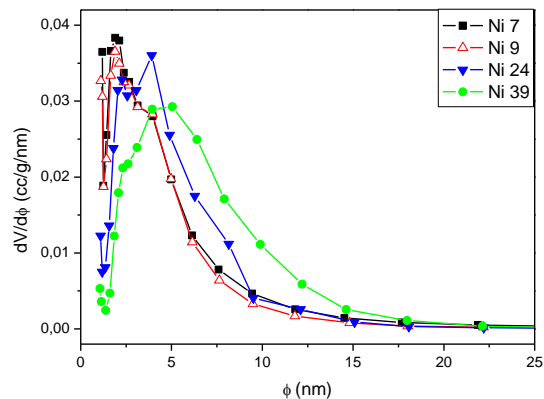


Fig. 1 Volume Pore Distribution of Calcined Samples.

Gelation times when adding nickel nitrate solution were much shorter than those observed in similar preparations using only HNO_3 as peptising agent. As nickel nitrate solution was incorporated before peptising of the boehmite was completed, the integration of Ni^{2+} ions in the matrix could proceed through a very close approximation to the boehmite particles. A much higher metal dispersion is expected relative to impregnation methods [22]. Another advantage of this modified sol-gel method is that accelerating the gelation process results in a greater gel volume.

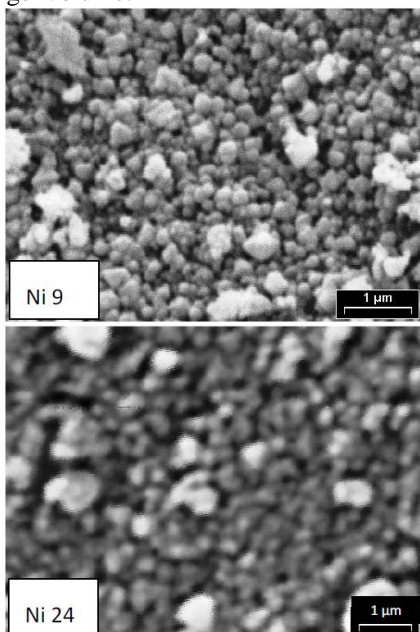


Fig. 2 SEM Photographs from Calcined Samples.

During calcination of already dry gels, the close proximity of Ni to aluminium hydroxide, allows a strong interaction between the metal and the support precursor. This way diffusion and sintering to produce larger Ni particles should not be favoured.

The homogeneous alumina structure observed by SEM together with these results demonstrated that samples with very high Ni loadings can be obtained by this method without losing specific area and porosity. In addition, the porous structure of the calcined material proved rather stable after complete reduction at 700°C , as indicated by the values of BET area from reduced samples listed in Table 1.

In Fig. 3, all XRD spectra for samples after calcination are shown. Besides the sample spectra the position of the most intense structures corresponding to NiO, spinel-like nickel aluminate, metallic Ni, and gamma-alumina are indicated. The presence of NiO in all samples was evident from these results. Pattern corresponding to $\gamma\text{-Al}_2\text{O}_3$ could also be observed. At first sight, there was not clear indication of structures matching nickel aluminate pattern; when analysing however, the two more intense diffraction peaks from gamma-alumina at 45.8° and 66.8° , it was possible to observe a shift of the peak maxima towards lower

angles. This effect was more important as the Ni content increased: Shifts from 45.8° in gamma-alumina to 45.4° in sample Ni 7, and to 45.0° in sample Ni 39 were determined. From this analysis it is possible to infer the presence of spinel-like nickel aluminate particles small enough to show not definite diffraction patterns. The size of the metal particle has been a troublesome aspect for catalysts and active membrane design. A general agreement among different authors indicates that high dispersed samples, i.e., with small metal particles are much more active and stable on stream [12]. NiO species are usually associated to larger metal particles. In our case, Ni 39 which is the sample with narrowest NiO pattern was used to estimate the NiO particle size; by means of the width of the 75.5° peak, 12 nm particles were evaluated.

A first treatment in reducing gas flow up to 800°C at $10^\circ\text{C}/\text{min}$ was conducted with the aim of identifying the different chemical states of Ni present in our samples. The results are presented in Fig. 4 as TG and DTG curves. In addition to humidity release about 150°C , two very well defined structures can be observed at 400°C and 700°C , approximately, which have been associated by other authors to reduction of NiO and spinel-like nickel aluminate particles, respectively [26].

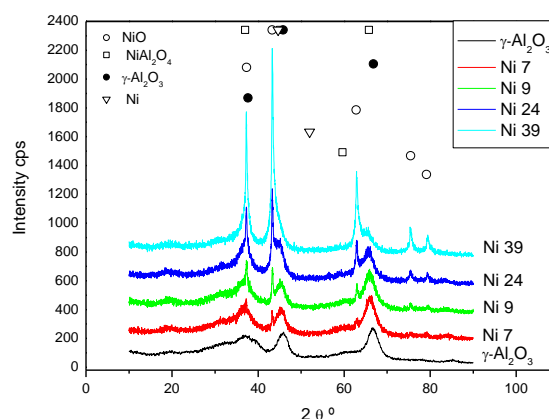


Fig. 3 XRD Spectra From Calcined Ni-Samples and Gamma Alumina.

The second structure at 700°C shifted towards lower temperatures as the Ni content increased. This shift is not completely evident from Fig. 4, but was confirmed by similar TG experiments on sample Ni 7 up to 1000°C (not shown). This indicates that in samples with lower Ni loadings, spinel NiAl_2O_4 species are more crystalline, their reduction temperature being closer to that reported for stoichiometric [27] and non-stoichiometric nickel aluminate [28]. A similar effect was observed by Kim et al. in $\text{Ni}/\text{Al}_2\text{O}_3$ [12] and by Guo et al. [29] in $\text{Ni}/\text{MgAl}_2\text{O}_4$ catalysts, where reduction temperature of the species produced by SMSI decreased from 800°C

to 705°C when nickel loading increased from 1 to 15%.

In order to confirm that the results shown in Fig. 4 were just due to reduction processes, two samples (Ni 9 and Ni 39) were analysed in a TG- MS set-up where in addition to mass changes, H₂O release was monitored. Results from the experience corresponding to sample Ni 9 are presented in Fig. 5.

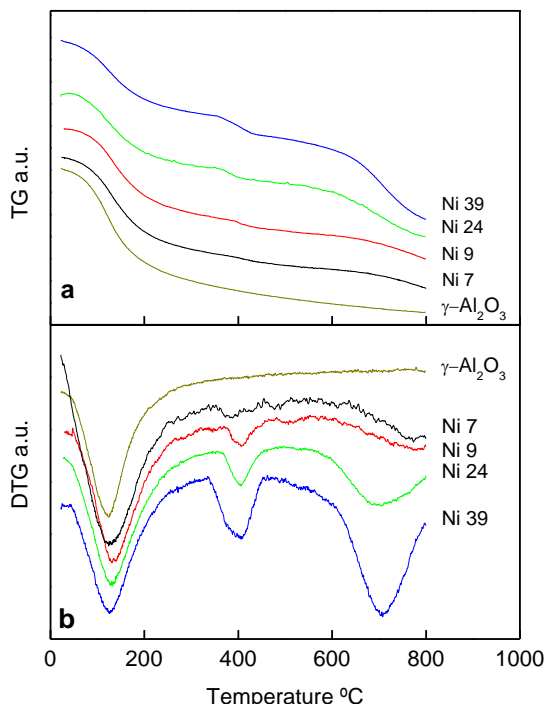


Fig. 4 TG (A) and Corresponding DTG (B) Curves After 800°C Treatment.

The H₂O curve showed three features at similar temperatures as those of Fig. 4.b), corresponding to sample humidity desorption and the two reduction stages described before.

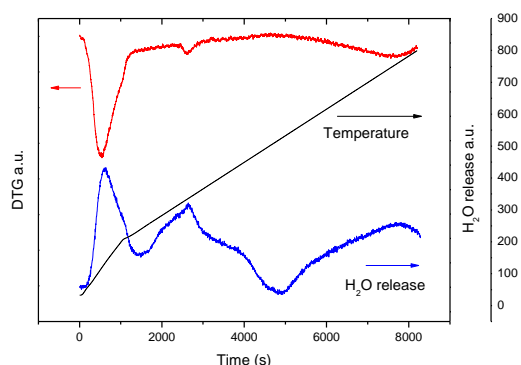


Fig. 5 DTG Curves From Calcined Sample Ni 9 Treated Up to 800°C And H₂O Release Measured Simultaneously By MS.

The presence of very small spinel-like NiAl₂O₄ particles, which was deduced from the shift of the diffraction peak at 45.8 ° in the XRD spectra

(Fig. 3), was confirmed by the two stage reduction scheme observed for all samples in reducing temperature treatments.

With the objective of only accomplishing the reduction of nickel oxide particles a treatment at 400°C was carried out in the STA set-up until no changes in mass were observed. Fig. 6 shows TG and DTG curves corresponding to these experiments. Two regions are indicated in this figure, one corresponding to the 1°C/min heating rate stage and the other to the 400°C plateau. From TG and DTG curves is evident that reducing flow at 400°C had no further effect on the samples under study after 30 min on stream (plateau). The XRD spectra recorded after this treatment are presented in Fig. 7. The peak at 52 ° originated from metallic Ni is clearly detected; this structure has the advantage of not overlapping any peak from other nickel compounds, acting as a fingerprint of the metallic state. Two aspects should be considered in relation to Fig. 7: spinel-like nickel aluminate can be observed as discussed in relation to calcined samples; on the other hand, contrary to what might be expected, NiO pattern was identified in treated samples. In Fig. 7 spectra, NiO reflections were evident for samples with higher Ni content as Ni 24 and Ni 39. Particle sizes estimated from these spectra were 3.5 nm for nickel aluminate, 7nm for NiO, and 20 nm metallic particles. Nickel aluminate and NiO particle sizes were obtained by means of multi-peak fitting of the overlapped structures. Although no sharp diffraction peak was observed, the presence of NiAl₂O₄ is plausible enough to justify its inclusion when fitting. A similar result has been presented by Kim et al. [11] in relation to very small particles not detectable by XRD in Ni/alumina aerogel catalysts.

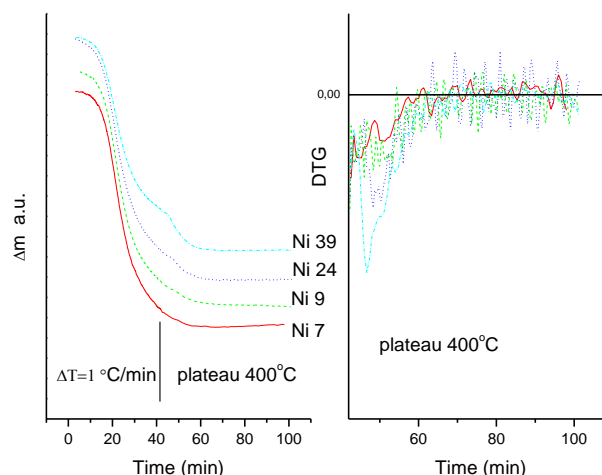


Fig. 6 TG And DTG Corresponding to the 400°C Plateau Treatment.

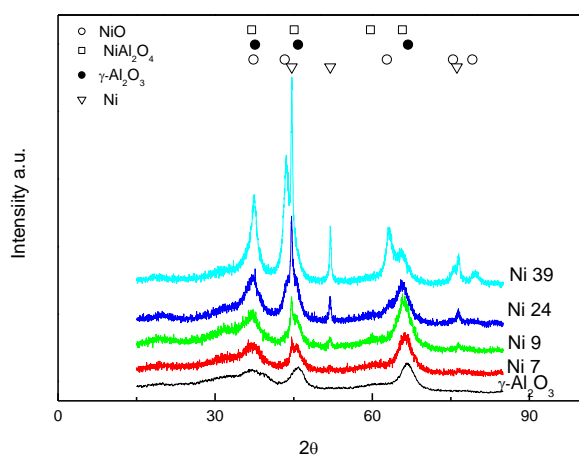


Fig. 7 XRD Spectra from Samples Treated at 400°C in H₂/Ar Flow.

In order to elucidate this argument, we analysed spectra obtained subtracting XRD γ -Al₂O₃ spectrum from every sample XRD spectrum; the resulting spectra are shown in Fig. 8. There is no way to separate completely the components corresponding to NiO and nickel aluminate; it is possible to observe however, that nickel aluminate structures are indeed broad enough to be originated by 3 nm particles.

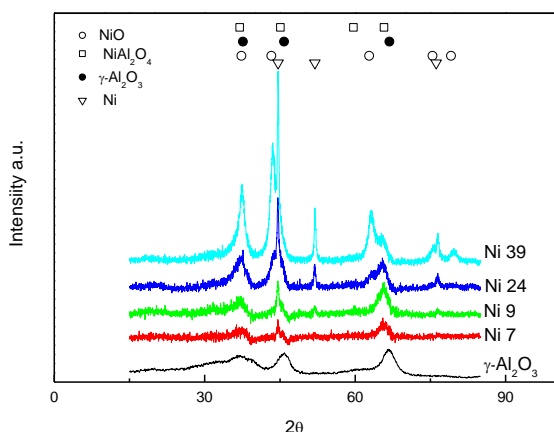


Fig. 8 XRD Spectra for Samples After 400°C Reduction, Obtained By Subtracting γ -Al₂O₃ XRD Spectrum.

After the last reducing treatment at 700°C, neither NiO nor NiAl₂O₄ could be detected in the XRD spectra for all samples but Ni 39, as displayed in Fig. 9, thus indicating that Ni particles are mainly arranged at the interstices between γ -Al₂O₃ agglomerates. This result is very important for the possible application of these materials as reactive ones, either as catalysts or membrane coatings, because it indicates that most of Ni will be accessible to reactive gases. Metal particle sizes in 700°C-reduced samples were evaluated from XRD spectra, 18 nm on average.

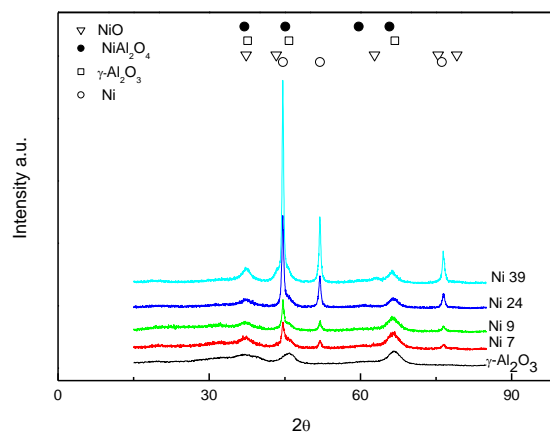


Fig. 9 XRD Spectra From Samples Treated at 700°C in H₂/Ar Flow.

As proceeded calculating difference spectra from samples after the 400°C treatments, in Fig. 10 difference spectra from all samples after 700°C treatments are shown. In this case, it is not possible to detect any other species than Ni⁰ in samples Ni 7, Ni 9, and Ni 24. The small signal at 37° and the tail towards lower angles in 45.8° Ni structure indicated that reduction was not completed in this sample. When checking the corresponding TG graphic, a very small deviation from null value was found in the TG derivative.

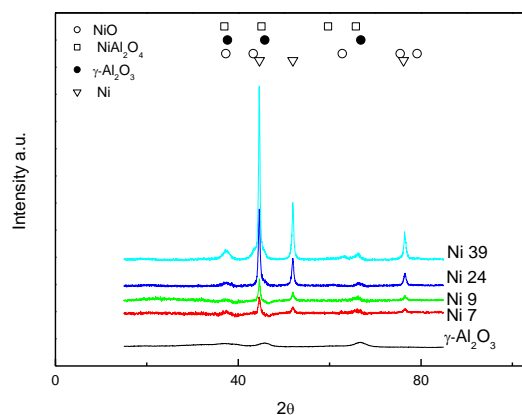


Fig. 10 XRD Spectra for Samples After 700°C Reduction, Obtained By Subtracting γ -Al₂O₃ XRD Spectrum.

Reduction treatment at 400°C is known to be effective in reducing NiO [29], it was also tested in our DTA-TG instrument set up with a pure NiO sample, which resulted almost completely (more than 95 wt%) reduced to Ni⁰ after 20 min of treatment. After a similar treatment, however, our samples had an important amount of NiO as indicated by XRD spectra. In principle, it could have been speculated about NiO particles immersed in bulk dense regions of the alumina matrix, inaccessible to reducing gas; the subsequent reduction of these structures during treatments at 700°C, which was determined by the

XRD characterisation, demonstrated, however, the presence in calcined samples of NiO species that were not reducible at a standard temperature. Evaluation of the particle size of these NiO structures gave values < 7 nm, significantly smaller than those particles found in calcined samples. Similar treatment at the temperature of reduction of spinel-like NiAl_2O_4 produced the total reduction of NiO in all samples. As mentioned above, the size for spinel-like NiAl_2O_4 particles in samples after reduction at 400°C ; were estimated to be not larger than 3.5 nm.

This anomalous behaviour of NiO species in the reduction reaction at 400°C can be explained in terms of strong metal alumina interaction at the surface of NiO particles, which favours the formation of a layer of nickel aluminate. Some XPS-AES results that will be published elsewhere, from samples prepared by sol-gel (12 h calcination) and by impregnation, showed the presence of spinel-like NiAl_2O_4 in calcined samples. The thickness of this aluminate layer was variable, depending on the Ni loading and the preparation method. In samples prepared by sol-gel and by impregnation with low Ni content, the aluminate layer remained long after long periods of Ar sputtering. On the contrary, in samples prepared by impregnation with Ni loading higher than 10%, were the NiO particles are expected to be larger, the aluminate layer was instable even to permanence in ultra-high vacuum and easily removed by Ar bombardment. In our case, larger NiO particles of 15 nm could be reduced at the standard NiO reduction temperature due to the instability of their very thin nickel aluminate outer layer. Intermediate NiO particles of 7nm should have a thicker aluminate layer, thus being more resistant to reduction but still reducible at 700°C . Very small particles of 3.5 nm or smaller formed by spinel-like NiAl_2O_4 species could also be reduced at 700°C . Maluf et al. have recently reported the presence of a high binding energy XPS peak corresponding to NiAl_2O_4 on the surface for samples prepared by coprecipitation [30].

SEM observations from the two samples with highest Ni content are shown in Fig. 11. In sample Ni 24 the gamma-alumina structure seemed to be modified when compared to that of the calcined sample (Fig. 2). Some aggregation of particles appears for both samples in SEM observations indicating the beginning of sintering after 700°C treatment.

All samples were observed by TEM; some photographs are presented in Fig. 12 to 13. All samples showed a homogeneous dispersion of Ni particles in a gamma-alumina matrix, with size-mean-value in the range of 20 - 30 nm, even for the sample with highest Ni content. These images give evidence of the possibility of preparing high dispersed Ni particles in the ceramic matrix regardless the Ni content.

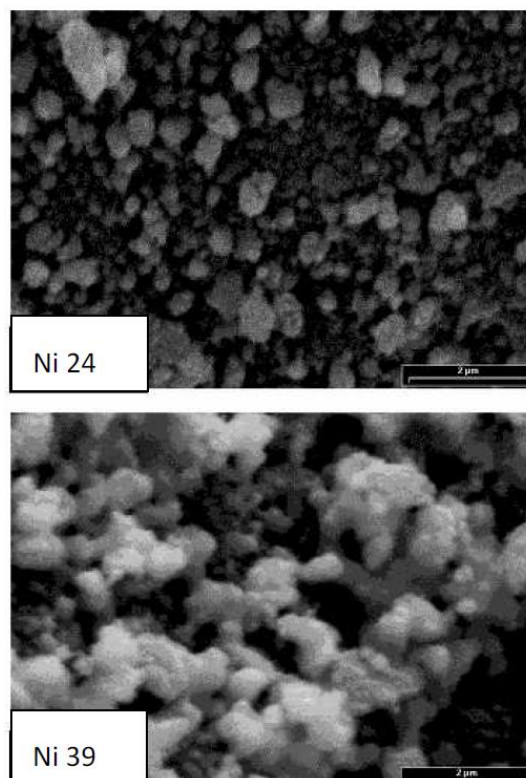


Fig. 11 SEM Photographs from Ni 24 and Ni 39 Reduced Samples.

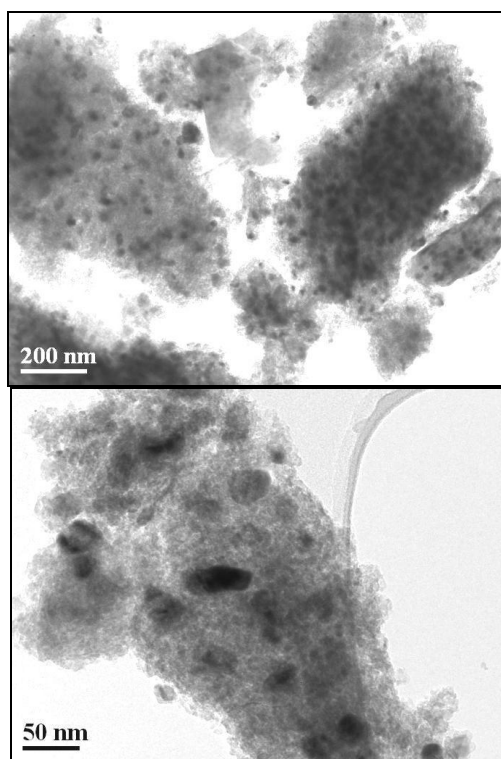


Fig. 12 TEM Photographs from Sample Ni 7.

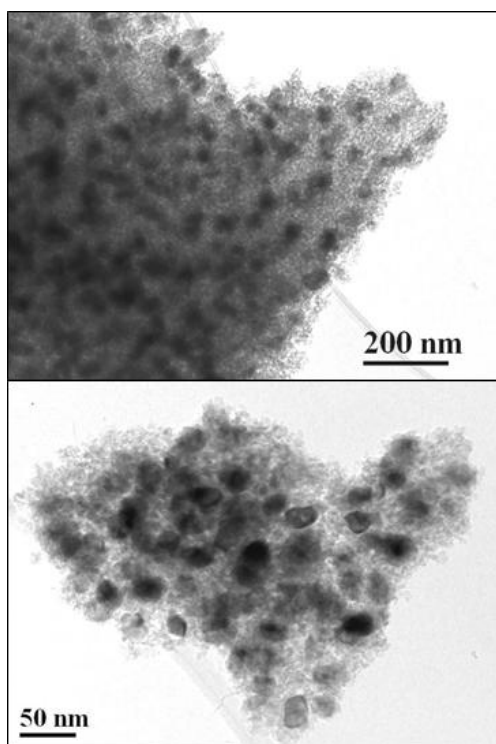


Fig 13 TEM Photographs from Sample Ni 24.

IV. CONCLUSIONS

The incorporation of the nickel salt solution at an early stage of the sol-gel process was demonstrated to accelerate gelation, thus favouring the nickel dispersion in the bohemite matrix. This allows obtaining samples with very high nickel content but still with high metal dispersion on an alumina support structure with very high specific area (128-170 m²/g), and small Ni-nanoparticles (<50nm) as indicated our nitrogen adsorption and TEM results. The preparation method favoured SMSI, responsible of the formation of spinel-like NiAl₂O₄ particles. In addition, these particles seemed were localised on the external surface and pore surface of the mesoporous alumina. This effect makes this material more interesting to be used as catalyst or reactive coating because the whole nickel content would be accessible for reaction.

Our combined experiments of reducing TG and XRD indicated that complete reduction of the Ni species was not possible at temperatures below 700°C, although at this temperature all nickel species transform to metallic Ni. This was accomplished, in most cases, in a reasonable short treatment time (30 min approx), thus avoiding sintering of nickel particles and any important decrease in the alumina specific area that, in our case, remained within 20% of the value from calcined samples.

Anomalous resistance to reduction at 400°C, observed for NiO species, was explained in terms of two different NiO-particle sizes and different degree of SMSI around them. Larger NiO particles of 20 nm

in size were probably covered by a thin aluminate-like layer as indicated previous studies in similar materials, smaller NiO particles of 7 nm in size were much less reducible due a to thicker aluminate surface layer. Once the aluminate-like reduction temperature was reached, at 700°C, all Ni species were reduced.

All samples showed particles of 20-30 nm in size under TEM, indicating that this method allows the obtention of high dispersed Ni particles even for high Ni contents.

ACKNOWLEDGMENTS

We are grateful to C. Osuna from INVAP SE for AAS determinations, and L.Dufou for XRD and SEM experiments.

MDS is grateful to CONICET for partial financial support.

REFERENCES

- [1] M. Prettre, CH. Eichner, M. Perrin, "The catalytic oxidation of methane to carbon monoxide and hydrogen," Trans. Faraday Soc., vol. 43, pp. 335-339, 1946.
- [2] W.J.M. Vermeiren, E. Blomsmaand, P.A. Jacobs, "Catalytic and thermodynamic approach of the oxyreforming reaction of methane," Catal. Today, vol. 13, pp. 427-436, 1992.
- [3] Abayomi J. Akande, Raphael O. Idem, Ajay K. Dalai, "Synthesis, characterization and performance evaluation of Ni/Al₂O₃ catalysts for reforming of crude ethanol for hydrogen production," Appl. Catal. A, vol. 287, pp. 159-175, 2005.
- [4] Shakeel Ahmeda, Abdullah Aitani, Faizur Rahman, Ali Al-Dawood, Fahad Al-Muhaish, "Decomposition of hydrocarbons to hydrogen and carbon," Appl. Catal. A, vol. 359, pp. 1-24, 2009.
- [5] Stéphane Haag, Michel Burgard, Barbara Ernst, "Beneficial effects of the use of a nickel membrane reactor for the dry reforming of methane: Comparison with thermodynamic predictions," J. Catalysis, vol. 252, pp. 190-204, 2007.
- [6] B.S. Liu, L.Z. Gao, C.T. Au, "Preparation, characterization and application of a catalytic NaA membrane for CH₄/CO₂ reforming to syngas," Appl. Catal. A, vol. 235, pp. 193-206, 2002.
- [7] P. Ferreira-Aparicio, I. Rodriguez-Ramos, A. Guerrero-Ruiz, "On the applicability of membrane technology to the catalysed dry reforming of methane," Appl. Catal. A, vol. 237, pp. 239-252, 2002.
- [8] Mitra Dadvar, Muhammad Sahimi, "The effective diffusivities in porous media with and without nonlinear reactions," Chem. Eng. Sci., vol. 62, pp. 1466-1476, 2007.
- [9] Chang-Yeol Yu, Bong-Kuk Sea, Dong-Wook Lee, Sang-Jun Park, Kwan-Young Lee, Kew-Ho Lee, "Effect of nickel deposition on hydrogen permeation behavior of mesoporous γ -alumina composite membranes," J. Colloid Interface Sci., vol. 319, pp. 470-476, 2008.
- [10] M.R. Othman, J. Kim, "Permeation characteristics of H₂, N₂ and CO₂ in a binary mixture across meso-porous Al₂O₃ and Pd-Al₂O₃ asymmetric composites," Microporous and Mesoporous Mater., vol. 112, pp. 403-410, 2008.
- [11] Jin-Hong Kim, Dong Jin Suh, Tae-Jin Park, Kyung-Lim Kim, "Effect of metal particle size on coking during CO₂ reforming of CH₄ over Ni-alumina aerogel catalysts," Appl. Catal. A, vol. 197, pp. 191-200, 2000.
- [12] Pil Kim, Younghun Kim, Heesoo Kim, In Kyu Song, Jongheop Yi, "Synthesis and characterization of mesoporous alumina with nickel incorporated for use in the partial oxidation of methane into synthesis gas," Appl. Catal. A, vol. 272, pp. 157-166, 2004.
- [13] Abayomi J. Akande, Raphael O. Idem, Ajay K. Dalai, "Synthesis, characterization and performance evaluation of

- Ni/Al₂O₃ catalysts for reforming of crude ethanol for hydrogen production,” *Appl. Catal. A*, vol. 287, pp. 159–175, 2005.
- [14] J. Juan-Juan, M.C. Román-Martínez, M.J. Illán-Gómez, “Nickel catalyst activation in the carbon dioxide reforming of methane. Effect of pretreatments,” *Appl. Catal. A*, vol. 355, pp. 27–32, 2009
- [15] X. Wang, G. Lu, Y. Guo, Y. Wang, Y. Guo, “Preparation of high thermal-stable alumina by reverse microemulsion method,” *Mater. Chem. Phys.*, vol. 90 225-229, 2005.
- [16] W. Deng, P. Bodart, M. Pruski, B.H. Shanks, “Characterization of mesoporous alumina molecular sieves synthesized by nonionic templating,” *Microporous and Mesoporous Mater.*, vol. 52 169-177, 2002.
- [17] X. Bokhimi, J. Sánchez-Valente, and F. Pedraza, “Crystallization of sol-gel boehmite via hydrothermal annealing,” *J. Solid State Chem.*, vol. 166, pp. 182-190, 2002.
- [18] K. Murata, K.M. Inaba, M. Miki, T. Yamaguchi, “Formation of filamentous carbon and hydrogen by methane decomposition over Al₂O₃-supported Ni catalysts,” *React. Kin. Catal. Lett.*, vol. 85, pp. 21–28, 2005.
- [19] Lingyu Piao, Yongdan Li, Jiuling Chen, Liu Chang, Jerry Y.S. Lin, “Methane decomposition to carbon nanotubes and hydrogen on an alumina supported nickel aerogel catalyst,” *Catal. Today*, vol. 74, pp. 145–155, 2002.
- [20] Guohui Li, Linjie Hu, Josephine M. Hill, “Comparison of reducibility and stability of alumina-supported Ni catalysts prepared by impregnation and co-precipitation,” *Appl. Catal. A*, vol. 301, pp. 16-24, 2006.
- [21] Zheng Xu, Yumin Li, Jiyan Zhang, Liu Chang, Rongqi Zhou, Zhanting Duan, “Bound-state Ni species - a superior form in Ni-based catalyst for CH₄/CO₂ reforming,” *Appl. Catal. A*, vol. 210, pp. 45–53, 2001.
- [22] J. Escobar, J.A. De Los Reyes, T. Viveros, “Nickel on TiO₂-modified Al₂O₃ sol-gel oxides: Effect of synthesis parameters on the supported phase properties,” *Appl. Catal. A*, vol. 253, pp. 151-163, 2003.
- [23] Z.X. Cheng, X.G. Zhao, J.L. Li, Q.M. Zhu, “Role of support in CO₂ reforming of CH₄ over a Ni/γ-Al₂O₃ catalyst,” *Appl. Catal. A*, vol. 205, pp. 31–36, 2001.
- [24] B. Yoldas, “Alumina Sol Preparation from Alkoxides,” *Am. Ceram. Soc. Bull.*, vol. 54, pp. 289-290, 1975.
- [25] G.L. Clark, *Applied X Ray*, 4th ed., Mc Graw Hill, NY 1955.
- [26] G. Goncalves, M.K. Lenzi, O.A.A. Santos, L.M.M. Jorge, “Preparation and characterization of nickel based catalysts on silica, alumina and titania obtained by sol-gel method,” *J. Non Cryst. Solids*, vol. 352, pp. 3697–3704, 2006
- [27] J.R. Rostrup-Nielsen, J.R. Anderson, M. Boudart (Eds.), *Catalysis, Science and Technology*, vol. 5, Springer, Berlin, 1984.
- [28] J.A. Peña, J. Herguido, C. Guimon, A. Monzón, J. Santamaría, “Hydrogenation of acetylene over Ni/NiAl₂O₄ catalyst: Characterization, coking, and reaction studies,” *J. Catal.*, vol. 159, pp. 313-322, 1996.
- [29] Jianjun Guo, Hui Lou, Hong Zhao, Dingfeng Chai, Xiaoming Zheng, “Dry reforming of methane over nickel catalysts supported on magnesium aluminate spinels,” *Appl. Catal. A*, vol. 273, pp. 75–82, 2004
- [30] S.S. Maluf, E.M. Assaf, “Ni catalysts with Mo promoter for methane steam reforming,” *Fuel*, vol. 88, pp. 1547-1553, 2009.